ESR and HRTEM Study of Carbon-Coated Nanocrystalline MgO

David S. Heroux,[†,‡] Alexander M. Volodin,[†] Vladimir I. Zaikovski,[†] Vladimir V. Chesnokov,[†] Alexander F. Bedilo,[‡] and Kenneth J. Klabunde*[,‡]

Boreskov Institute of Catalysis, Novosibirsk 630090, Russia, and Department of Chemistry, Kansas State University, Manhattan, Kansas 66506

Received: August 5, 2003

Carbon-coated nanocrystalline MgO samples were prepared by butadiene pyrolysis at 500 °C over aerogel-prepared MgO samples. Samples with carbon loadings of 1.2, 3.2, 5.0, 10.0, and 15.9 wt % were prepared. Initial carbon formation rate was about 2 wt % per hour. According to HRTEM, the structure of the mineral component in the carbon-mineral materials was not altered by the carbon deposition. At low loading of carbon, it was found to deposit only inside the MgO aggregates 5−10 nm from their outside surface, forming thin individual bands 1.5−2 nm long. At the highest loading, carbon deposits form three-dimensional graphite-like multilayer structures filling the pore volume of the MgO aggregates and cover the outside surface of the aggregates with a thin monolayer coating. A single symmetric Lorentzian line with $g = 2.0029$ attributable to carbon deposits has been observed in the ESR spectra of the carbon-mineral materials. It gradually narrows from 5.0 to 1.9 G as the carbon loading increases from 1.2 to 15.9 wt %. Nitroxyl radicals formed after dinitrobenzene adsorption on MgO nanocrystals have been used as a spin probe for estimation of the concentration of strong basic sites present on the surface of the carbon-mineral materials and degree of their coverage with carbon. The sample with the carbon loading of 15.9 wt % has practically all such sites blocked with carbon, while samples with carbon concentration between 5 and 10 wt % seem to be the most promising candidates for practical application as destructive adsorbents.

Introduction

Nanocrystals of common metal oxides such as MgO, CaO, ZnO, TiO_2, Al_2O_3, and Fe_2O_3, have been shown to be highly efficient and active adsorbents for many toxic chemicals including air pollutants, chemical warfare agents, and acid gases [refs 1−6 and references therein]. In most cases, destructive adsorption takes place on the surface of the nanocrystals, so that the adsorbate is chemically dismantled and thereby made nontoxic. In particular, aerogel-prepared (AP) nanocrystalline MgO has been shown to have small average particle size (∼4 nm), high surface area (>500 m^2/g), and high reactivity.[1,7]

The use of these nanocrystalline metal oxides, especially AP-MgO, is limited under conditions where liquid water or water vapor is present due to their tendency to adsorb water, and thereby be partially deactivated toward adsorption of the target pollutants. Activated carbon is made up of mainly graphitic structures, which exhibit a less polar surface, and the tendency to adsorb water is lessened compared with nanocrystalline metal oxide surfaces. Recently we have shown that deposition of a partial carbon coating over nanocrystalline MgO may have a significant beneficial effect on its performance as a destructive adsorbent.[8]

Carbon-mineral materials (CMMs) are used in various applications of catalysis, biocatalysis, and adsorption. These materials have the so-called mosaic-like surface structure with simultaneous availability of both hydrophilic (mineral) and hydrophobic (carbon) phases on their surface. One of the traditional methods of CMMs preparation is carbon deposition by pyrolysis of various gaseous carbonaceous precursors at 500−900 °C over the surface of a mineral support. Such a method is usually referred to as carbon chemical vapor deposition (CVD). Particular surface hydrophilic/hydrophobic composition depends on preparation conditions as well as the type of the mineral compound.

In this study we have prepared carbon-coated AP-MgO samples by pyrolysis of butadiene at 500 °C. This is a relatively fast and efficient method for deposition of carbon on a mineral support.[9] Prepared materials were characterized by HTREM and ESR using dinitrobenzene as a spin probe. Its adsorption on magnesium oxide and other oxide materials with sufficiently strong electron-donor (basic) sites results in the formation of nitroxyl radicals.[10,11] Since the carbon coating does not have such sites, the concentration of radicals formed over carbon-coated AP-MgO can be used to determine the percentage of surface basic sites remaining available after depositing different amounts of carbon.

Experimental Section

Reagents and Materials. Preparation of aerogel-prepared (AP) MgO has been covered in detail elsewhere.[1,7] Briefly, AP-MgO was prepared from a magnesium methoxide precursor in a methanol−toluene solution. Dropwise addition of deionized water, with vigorous stirring for several hours, forms a hydroxide gel. This gel is dried of the solvents in an autoclave under supercritical conditions. The obtained hydroxide was heated slowly to 480 °C and kept at that temperature overnight. The resulting material possessed a surface area of 520 m^2/g.

* Author to whom correspondence should be addressed: Dr. Kenneth Klabunde, University Distinguished Professor. Phone: 785-532-6829. Fax: 785-532-6666. E-mail: kenjk@ksu.edu.
[†] Boreskov Institute of Catalysis.
[‡] Kansas State University.

10.1021/jp036307c CCC: $27.50
Published on Web 02/12/2004

Carbon Formation. A flow reactor equipped with a Mcbain spring balance was used for carbon formation. AP-MgO was placed in a quartz basket and placed on a spring. This allowed for measuring of the sample weight change and accurate determination of carbon percentage in the sample. Then, the sample was heated under a flow of argon, at 500 °C for 1 h. After that, butadiene used as a carbon source was added to the flow. The flow rates were as follow: butadiene, 7.5 L/h; argon, 75 L/h. Initial carbon formation occurred at a rate of approximately 2 wt % per hour. The carbon loadings obtained for AP-MgO samples were 1.2, 3.2, 5.0, 10.0, and 15.9 wt %. After the desired amount of carbon was obtained, the butadiene flow was stopped and the product was cooled to room temperature under an argon flow, 75 L/h. The cooled samples were weighed and transferred to an airtight vial. To have a proper reference point for the investigation of basic sites, a blank sample containing no carbon was prepared by heating an original AP-MgO sample to 500 °C under argon for 1 h without butadiene.

Characterization of Basic Sites by ESR. Approximately 10 mg of sample (weighed on an analytical balance) was used for each experiment. Each sample was placed into a standard borosilicate glass ESR tube. The samples were degassed at room temperature for 30 min and then at 500 °C for another 30 min. After the heat treatment, the samples were allowed to cool to room temperature. Then, the tubes were flame-sealed to ensure that the sample remained under vacuum. Carbon spectra were recorded for each sample under vacuum. Basic sites were tested using 1×10^{-2} M dinitrobenzene (DNB) solution in dried toluene. The tubes were opened and approximately 0.2 mL of this solution was added to each sample. This amount ensured that the tubes were filled 1 cm above the height of the sample and that excess DNB was present. The tubes were then flame-sealed to limit exposure to the atmosphere. X-band ESR spectra were registered at room temperature using an ERS-221 spectrometer. Homemade computer programs (EPR-CAD) were used for processing of the experimental data.

HRTEM Characterization of Samples. Carbon-coated AP-MgO samples with 3.2 and 15.9 wt % carbon were studied by a high-resolution transmission electron microscope (HTREM) on a JEM-2010 instrument (JEOL, Japan) with lattice resolution 1.4 Å and accelerating voltage 200 kV. Selected area diffraction (SAD) was used for the phase identification. Samples for microscopy were prepared by suspending the powders in ethanol with the following ultrasound treatment (≤ 5 W/cm^2). Then, an aerosol created from the suspension was deposited on thin supports. Holey amorphous carbon films with the thickness of 10−20 nm supported on standard copper grids were used as the supports.

Results and Discussion

HRTEM Study. The structure of MgO in C/MgO is similar in all aspects to that of AP-MgO described earlier.[3,12] AP-MgO consists of 10−60 Å crystallites arranged into chains forming a very porous network. Note that the aggregates in AP-MgO are formed by interlacing extended chains of MgO nanocrystals and have the parallelepiped shape. Such organization of the aggregates presumes that they have a well-developed system of pores.

In HRTEM images of 3.2 wt % C/MgO sample (Figure 1) carbon deposits can be observed only inside the MgO aggregates 5−10 nm from their outside surface (arrows Figure 1b.). Here one can see thin contrast individual bands 1.5−2 nm long. These bands correspond to the side projections of very small graphite layers—two-dimensional carbon deposits. MgO nanoparticles located on the surface of the aggregates have clean surfaces and do not contain carbon. One can clearly see a system of MgO crystallographic planes (200) and (220).

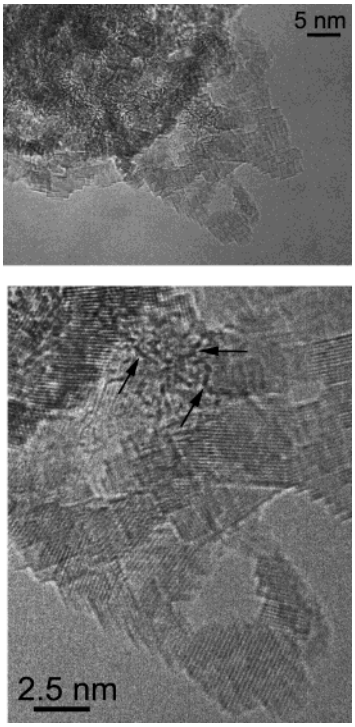

Figure 1. (a) HRTEM micrograph of AP-MgO coated with 3.2% carbon, (b) higher magnification showing clearly defined carbon layer.

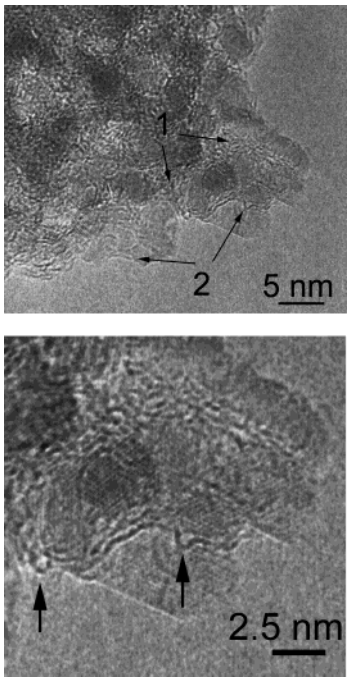

Figure 2. (a) HRTEM micrograph of AP-MgO coated with 15.9% carbon, (b) higher magnification image.

Carbon deposits in the 15.9% C/MgO sample (Figure 2) are very different. Here carbon is present both inside the MgO aggregates and on their surface (shown with arrows (1) and (2) in Figure 2a). However, the carbon deposits in these locations have different character. Inside the aggregates carbon forms multilayer graphite-like enclosures (1) that are interconnected with each other and fill the pores between MgO nanoparticles.

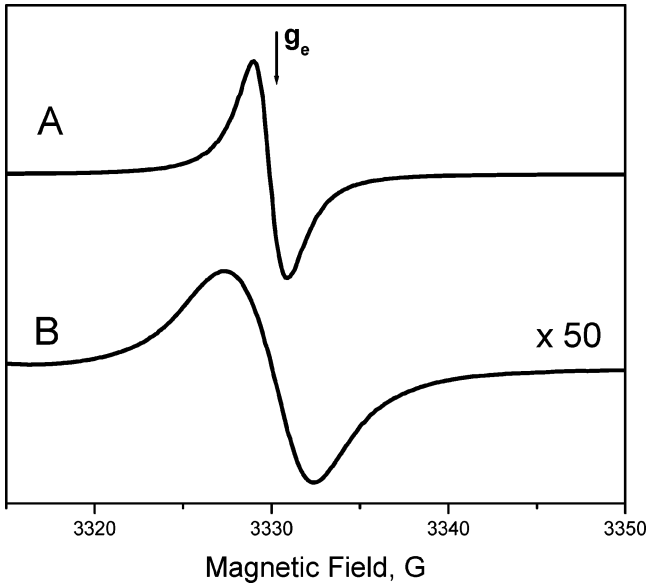

Figure 3. Comparison of the ESR spectra of carbon-containing MgO samples before adsorption of dinitrobenzene. Carbon loadings are 15.9 wt % (A), and 1.2 wt % (B).

These carbon enclosures can be called three-dimensional. In these cases the distances between the monolayers are 0.35−0.4 nm. This is close to the interplanar distance in graphite $d_{002} = 0.34$ nm. The typical thickness of these carbon deposits is 1−2 nm. As a rule, these graphite-like monolayers are parallel to the surface of MgO nanocrystals. However, in some cases diversion from parallelism accompanied by significant disordering of the structure of carbon deposits takes place.

On the surface of the aggregates the carbon coating is two-dimensional (2), and its thickness is down to a single graphite-like monolayer. Most of the MgO surface is covered with carbon. However, some MgO nanocrystals still have part of their surface not covered. The analysis of the morphology of the monolayers covering the surface of MgO nanocrystallites has shown that in many cases they are distorted with the formation of closed fullerene-like bubbles about 0.5 nm in diameter shown with arrows in Figure 2b. The fullerene-like bubbles on a carbon monolayer seem to be nuclei for the growth of additional layers during the formation of multilayer graphite-like structures.

One can suppose that the preferential filling of the internal pores of the MgO aggregates with carbon is due to the presence of some functional groups capable of anchoring hydrocarbon molecules during carbonization. Such anchors can also be formed by carbon bound to the surface of AP-MgO support during the preparation procedure. Whatever the nature of the anchors, they are probably not present on the surface of the aggregates, as clean MgO surface is known to adsorb hydrocarbons very weakly.

ESR Study. An ESR spectrum of AP-MgO without carbon after the pretreatment in flowing argon at 500 °C did not show any ESR signal, except for a weak typical Mn^{2+} signal present as an impurity in most MgO samples. In particular, it is important to note that ESR signals of $-O-CH_2$ radicals and F^+ sites recently reported by us to be present on as-prepared AP-MgO[13] are no longer observable. We attribute this fact to the presence of minute oxygen impurities in argon that led to oxidation of the MgO(OCH_2) surface.

ESR spectra of all MgO samples treated with butadiene exhibited a single line of varying width and intensity with the *g* factor close to 2.0029 and shape close to Lorentzian. Figure 3 presents ESR spectra of samples with 1.2 and 15 wt % carbon.

TABLE 1: ESR Examination of Basic Sites on Carbon-Containing AP-MgO Samples

carbon loading, wt %	width of the carbon peak, G	relative intensity of the DNB component	concentration of basic sites, sites/g	percentage of MgO basic sites tested by DNB, %
0		9.5	2.3E + 18	100
1.2	5.0	6.1	1.9E + 18	83
3.2	3.5	4.1	1.7E + 18	74
5	3.6	2.7	9.6E + 17	42
10	2.8	0.7	2.3E + 17	10
15.9	1.9	0	0	0

The width of this signal goes down from 5.0 to 1.9 G as the amount of carbon increases from 1.2 to 15 wt % (Table 1).

Similar ESR signals are well-known for carbonization products on the surface of catalytic materials.[14] The width of the ESR line attributed to carbonization products is mostly determined by the dipole interactions of unpaired electrons with magnetic moments of residual hydrogen atoms and with other unpaired electrons.[15] These two effects lead to line broadening due to the contributions of unresolved hyperfine structure and spin−spin broadening, respectively.

On the other hand, strong exchange between the unpaired electrons and delocalization of the unpaired electron over large systems of conjugated chemical bonds are known to result in narrowing of the ESR line.[15] Such narrowing usually corresponds to an increase of the size of carbon structures due to an increase of the carbonization temperature or longer treatment at a high temperature. In our case, the narrowing of the line with the growth of the carbon loading appears to indicate the formation of larger carbon particles in samples with higher carbon loadings. This fact agrees well with the above HRTEM observation of three-dimensional carbon deposits in the sample with 15 wt % carbon. Meanwhile, these deposits remain fairly small due to size restrictions inside the MgO aggregates. As a result, the ESR line does not become very narrow. For comparison, line widths smaller than 1 G are known for carbonized chars.[16]

Basic surface sites can be studied by ESR using the adsorption of aromatic nitrocompounds. If sufficiently strong electron-donor (basic) sites are present on the surface, their adsorption is accompanied by the formation of paramagnetic particles. The radicals appearing after adsorption of initially diamagnetic nitrocompounds were traditionally assumed to be their radical anions.[17,18] Later, on the basis of their spectral parameters, the spectra were assigned to surface-stabilized nitroxyl radicals resulting from the transformations in the initial radical pairs.[10,11]

$$NB + \mathbf{D}_s \leftrightarrows [NB\bullet\, \mathbf{D}_s] \rightleftarrows [NB^{-\bullet}\, \mathbf{D}_s^{+}]^{*} \rightarrow \bullet\mathbf{R}_{st}$$

The above scheme illustrates all stages of this process. First, an organic nitrocompound (NB) is adsorbed on a surface donor site ($\mathbf{D}_s$) to form a donor−acceptor complex [NB• $\mathbf{D}_s$]. The second stage represents reversible excitation of such complex either in a thermal process or due to illumination. With some probability the excited complex can then undergo a chemical reaction to give a stable nitroxyl radical •$\mathbf{R}_{st}$.

Besides MgO and Al_2O_3 studied most frequently, other oxide materials with strong basic sites, such as CaO, SrO, BaO, and TiO_2, have been shown to be capable of nitrobenzene reduction to the nitroxyl radicals.[19] The sites where this reaction takes place are known to be basic since they could be deactivated by Lewis and Bronsted acids and other molecules reacting with basic sites (CO_2, H_2O, H_2S, HCl, CS_2, etc.). Since strong basic sites are believed to account for the unique properties of

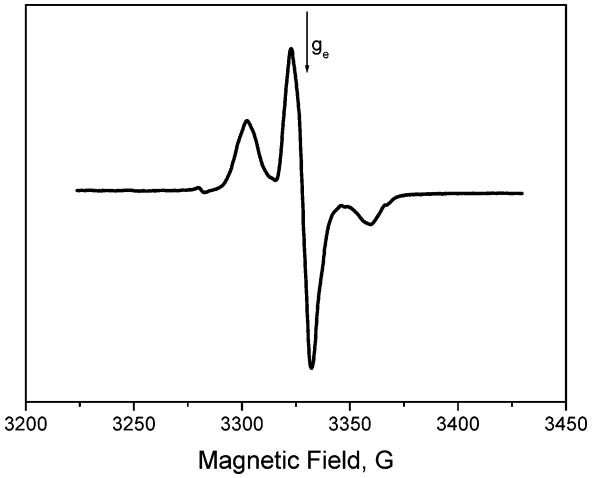

Figure 4. ESR spectrum of AP-MgO after adsorption of dinitrobenzene.

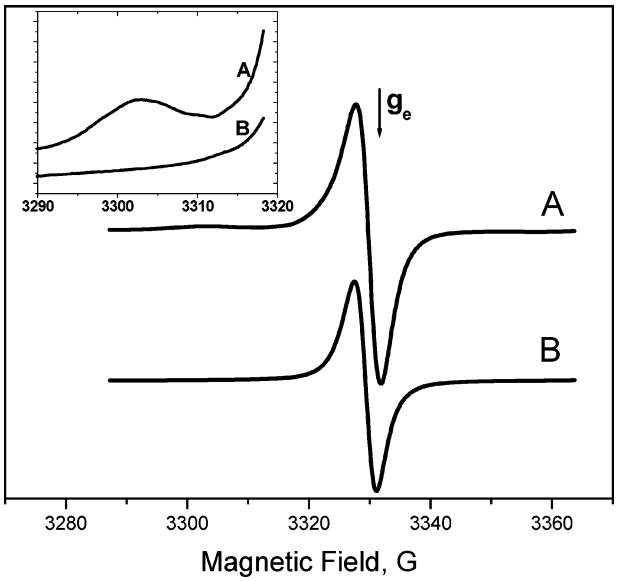

Figure 5. ESR spectra for AP-MgO containing 5 wt % carbon. (A) After dinitrobenzene adsorption; (B) before dinitrobenzene adsorption.

nanocrystalline alkaline earth metal oxides as destructive adsorbents, the formation of radicals after DNB adsorption appeared to be a convenient technique for determination of their concentration over AP-MgO partially coated with carbon.

Figure 4 shows a typical three-component spectrum of nitroxyl radicals formed after DNB adsorption over AP-MgO with $g = 2.0038$ and $A_{zz} = 28.5$ G. The shape of the spectrum is due to hyperfine splitting on a nitrogen atom and frozen rotation. The spectra of all samples after DNB adsorption were recorded the next day approximately in 24−26 h after DNB was added to the samples, since the formation of nitroxyl radicals from DNB is a relatively slow process at room temperature without illumination. Earlier this time was found sufficient to reach the maximum concentration of the nitroxyl radicals over AP-MgO.[13] Double integration of this spectrum gives us the concentration of basic sites capable of reducing DNB to nitroxyl radicals, which is equal to 2.3×10^{18} sites/g. Interestingly, this concentration is remarkably close to that earlier observed over the same material after activation in air.[13]

Figure 5 presents ESR spectra of AP-MgO with 5 wt % carbon before (B) and after (A) DNB adsorption. One can see that the ESR spectra of carbon-coated AP-MgO are still dominated by the carbon signal discussed above. This signal

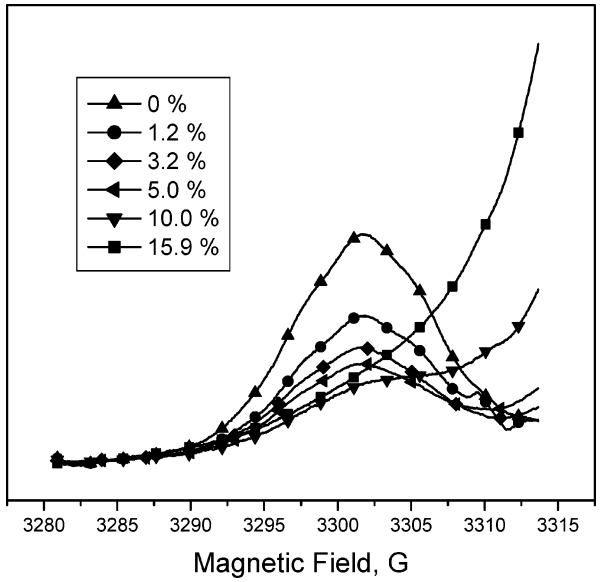

Figure 6. ESR spectra for AP-MgO containing various percentages of carbon after adsorption of dinitrobenzene.

does not change much after the DNB adsorption. Although the central component of the ESR spectra of nitroxyl radicals formed from DNB overlaps this signal, the intensity of the latter is much higher for all samples, except for the sample with 1.2 wt % carbon where the two are comparable.

The best way to distinguish the ESR spectra of carbon-coated samples before and after adsorption is by looking at the low-field component in the spectrum of nitroxyl radicals shown in magnified scale in the inset to Figure 5. Although the strong carbon signal still contributes to the baseline in this spectral region, the contributions of the two signals can be easily separated for this sample. While double integration of the whole DNB spectrum is clearly not possible, relative intensities of this signal over different samples should be proportional to the integral intensity of this component.

We took advantage of this opportunity to determine the concentrations of strong basic sites over carbon-coated AP-MgO samples. Figure 6 shows the spectral region corresponding to this component in the ESR spectra of all carbon-coated samples. The intensity of the spectrum of nitroxyl radicals formed from DNB clearly goes down as the carbon loading increases. Meanwhile, the contribution of the carbon line goes up. In the spectra of the samples with 5 wt % carbon or less, the two lines can be separated without any problem. This allows for accurate integration of the DNB component. This component is still clearly visible in the spectrum of the sample with 10 wt % carbon, although the relative error in its quantification is much higher in this case.

Finally, the spectrum of the sample with 15.9 wt % carbon does not have this line at all. We think this is indicative of the absence of strong basic sites capable of generating nitroxyl radicals from DNB on the surface of this material. This conclusion is in excellent agreement with our HRTEM data, which indicates that almost all the surface of this material is covered with carbon. Open MgO sites are very scarce and would not be noticed in the ESR spectrum.

Results of the quantitative analysis of these spectra are reported in Table 1. Here the third row gives information on relative integral intensities of the component of the DNB spectrum as shown in Figure 6. Specific concentrations of basic sites reported in fourth row were calculated from the relative intensities with the account of the sample weights using the

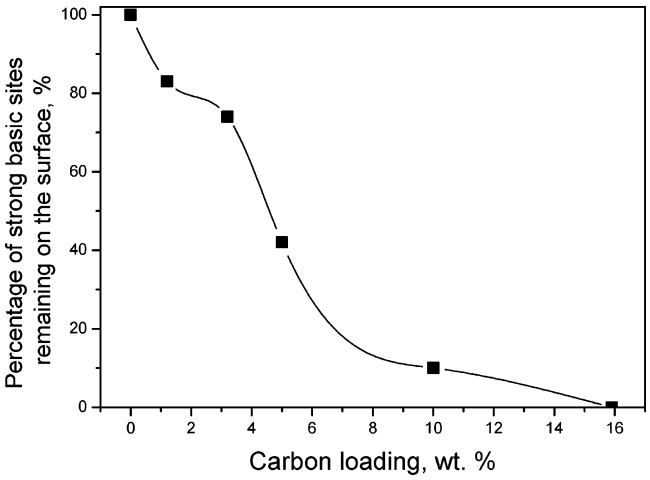

Figure 7. Dependence of the percentage of open basic sites on the surface of carbon-coated AP-MgO on the carbon loading.

absolute concentration of such sites over AP-MgO. If this initial concentration is taken as 100%, the ratio of the concentrations of basic sites over carbon-coated samples to this value corresponds to the percentage of such sites remaining after the carbon deposition.

The dependence of this percentage on the concentration of carbon is presented in Figure 7. This dependence is essentially not linear. We believe that this is due to the earlier observation of different places of carbon localization. As it is suggested by the HRTEM data, at low carbon loadings (3.2 wt % or less) carbon is primarily deposited inside the MgO aggregates, while most of the surface is free from carbon. It is quite natural that most of the surface basic sites are free from carbon as well and can participate in chemical reactions.

Apparently, covering of the main part of the MgO surface with carbon occurs between 3 and 10 wt % carbon. By 15 wt % carbon, the formation of a thin carbon coating over the MgO aggregates is practically complete, so the active sites are no longer accessible for reactants. From a practical point of view, one can expect samples with 5 to 10 wt % carbon to be the most interesting. They still have a considerable fraction of active sites available for adsorption, while a significant part of their surface is already coated with carbon that can help to prevent deactivation of the adsorbents, for example by water vapor.

Conclusion

The ESR technique with the use of dinitrobenzene as a spin probe suggested in this paper appears to be a very effective tool for investigation of nanocrystalline alkaline earth metal oxides partially covered with carbon. The analysis of the low field component in the spectrum of nitroxyl radicals formed from DNB allows for quantitative determination of the concentration of strong basic sites present on the surface of such carbon-mineral materials and degree of their coverage with carbon. It is a relatively fast and easy method that can be recommended for use in all cases when it is important to estimate the fraction of the surface of solid bases covered with carbon or other coatings that do not have strong basic sites.

The HRTEM data show that the carbon deposition method used in this study does not alter the structure of nanocrystalline magnesium oxide. Carbon is first deposited inside the pore volume of the aggregates while their surface is covered only after the pores are filled with carbon. Materials with intermediate carbon loadings between 5 and 10 wt % are very promising candidates for use as carbon-mineral destructive adsorbents. Their study in various destructive adsorption reactions of practical interest will be continued in our laboratories. There is also the possibility that some adsorbates could be adsorbed by the carbon and then slowly diffuse through to the MgO reactive sites. Therefore, further studies of destructive adsorption while comparing the different carbon loadings will be of considerable interest, since selectivities as well as activities will be altered compared with non-carbon coated MgO nanocrystals.

Acknowledgment. This study has been supported by the U.S. Army Research Office, CRDF (Project RC1-2340-NO-02), the Russian Foundation for Basic Research (Grant 03-03-33178), and Russian Department of Industry and Science (Grants SS-2120.2003.3 and SS-1140.2003.3).

References and Notes

(1) Klabunde, K. J.; Stark, J. V.; Koper, O. B.; Mohs, C.; Park, D. G.; Decker, S.; Jiang, Y.; Lagadic, I.; Zhang, D. *J. Phys. Chem.* **1996**, *100*, 12142.

(2) Koper, O. B.; Lagadic, I.; Volodin, A.; Klabunde, K. J. *Chem. Mater.* **1997**, *9*, 2468.

(3) Richards, R.; Li, W.; Decker, S.; Davidson, C.; Koper, O.; Zaikovski, V.; Volodin, A.; Rieker, T.; Klabunde, K. J. *J. Am. Chem. Soc.* **2000**, *122*, 4921.

(4) Wagner, G. W.; Koper, O. B.; Lucas, E.; Decker, S.; Klabunde, K. J. *J. Phys. Chem. B* **2000**, *104*, 5118.

(5) Carnes, C. L.; Klabunde, K. J. *Langmuir* **2000**, *16*, 3764.

(6) Carnes, C. L.; Kapoor, P. N.; Klabunde, K. J.; Bonevich, J. *Chem. Mater.* **2002**, *14*, 2922.

(7) Utamapanya, S.; Klabunde, K. J.; Schlup, J. R. *Chem. Mater.* **1991**, *3*, 175.

(8) Bedilo, A. F.; Sigel, M. J.; Koper, O. B.; Mel'gunov, M. S.; Klabunde, K. J. *J. Mater. Chem.* **2002**, *12*, 3599.

(9) Buyanov, R. A. *Coke Formation on Catalysts*; Nauka: Novosibirsk, 1983 (in Russian).

(10) Konovalova, T. A.; Volodin, A. M.; Chesnokov, V. V.; Paukshtis, E.; Echevskii, G. V. *React. Kinet. Catal. Lett.* **1991**, *43*, 225.

(11) Volodin, A. M.; Bolshov, V. A.; Konovalova, T. A. *Mol. Eng.* **1994**, *4*, 201.

(12) Mishakov, I. V.; Bedilo, A. F.; Richards, R. M.; Chesnokov, V. V.; Volodin, A. M.; Zaikovskii, V. I.; Buyanov, R. A.; Klabunde, K. J. *J. Catal.* **2002**, *206*, 40.

(13) Richards, R. M.; Volodin, A. M.; Bedilo, A. F.; Klabunde, K. J. *Phys. Chem. Chem. Phys.*, submitted.

(14) Kalinina, N. G.; Poluboyarov, V. A.; Anufrienko, V. F.; Ione, K. G. *Kinet. Katal.* **1986**, *27*, 237.

(15) Tikhomirova, N. N.; Lukin, B. V.; Razumova, L. L.; Voevodskii, V. V. *Doklady Akademii Nauk SSSR* **1958**, *122*, 264.

(16) Mrozowski, S.; Gutsze, A. *Carbon* **1977**, *15*, 335.

(17) Flockhart, B. D.; Leith, I. R.; Pink, R. C. *Trans. Faraday. Soc.* **1970**, *66*, 469.

(18) Flockhart, B. D.; Megarry, M. C.; Pink, R. C. *Adv. Chem.* **1973**, *121*, 509.

(19) Morris, R. M.; Klabunde, K. J. *Inorg. Chem.* **1983**, *22*, 682.